Solid-State Dynamics of Uranyl Polyoxometalates

Citation	Alam, T. M., Liao, Z., Zakharov, L. N. and Nyman, M. (2014). Solid-State Dynamics of Uranyl Polyoxometalates. Chemistry: A European Journal, 20: 8302–8307. doi:10.1002/chem.201402351
DOI	10.1002/chem.201402351
Publisher	John Wiley & Sons Ltd.
Version	Version of Record
Terms of Use	http://cdss.library.oregonstate.edu/sa-termsofuse

ChemPubSoc Europe

DOI: 10.1002/chem.201402351

CHEMISTRY
A European Journal
Communication

Polyoxometalates

Solid-State Dynamics of Uranyl Polyoxometalates

Todd M. Alam,*[a] Zuolei Liao,[b] Lev N. Zakharov,[b] and May Nyman*[b]

Abstract: Understanding fundamental uranyl polyoxometalate (POM) chemistry in solution and the solid state is the first step to defining its future role in the development of new actinide materials and separation processes that are vital to every step of the nuclear fuel cycle. Many solid-state geometries of uranyl POMs have been described, but we are only beginning to understand their chemical behavior, which thus far includes the role of templates in their self-assembly, and the dynamics of encapsulated species in solution. This study provides unprecedented detail into the exchange dynamics of the encapsulated species in the solid state through Magic Angle Spinning Nuclear Magnetic Resonance (MAS NMR) spectroscopy. Although it was previously recognized that capsule-like molybdate and uranyl POMs exchange encapsulated species when dissolved in water, analogous exchange in the solid state has not been documented, or even considered. Here, we observe the extremely high rate of transport of Li^+ and aqua species across the uranyl shell in the solid state, a process that is affected by both temperature and pore blocking by larger species. These results highlight the untapped potential of emergent f-block element materials and vesicle-like POMs.

Metal–oxo cluster chemistry is expanding into unprecedented territory, yet it is always dominated by the metal cations with the predominant aqueous 'yl'-state, meaning high valence with one or more multiply bonded oxo ligands.[1] The multiply bonded oxo ligand (double or triple bonded) is relatively inert to hydrolysis and condensation reactions, and thus stabilizes the surface of discrete metal–oxo clusters so that it remains water soluble without ancillary protecting ligands. Metal–oxo cluster chemistry is dominated by polyoxometalates (POMs) of the early d^0 transition metals (V, Nb, Ta, Mo, and W), the chemistry of which has been known since the late 1800s.[2] On the other hand, the uranyl cation, $U^{VI}O_2^{2+}$, that carries two *trans* yl-oxo ligands has only relatively recently (2005) been assembled into POMs.[3] With the *trans* yl-oxo configuration, the uranyl POMs are actually hollow capsules; the yl-oxygen stabilizes both the surface of the cluster and the inner surface of the uranyl shell. This ubiquitous capsule-like morphology leads to fascinating behavior as the encapsulated species (water, cations, and anions) not only template the capsule assembly,[4] but subsequently exchange with the exterior aqueous environment.[5]

One of the first discovered uranyl POMs was U_{24},[3] composed of 24 uranyl dihydroxide diperoxide polyhedra with the formula $[UO_2(O_2)(OH)]_{24}^{24-}$ (Figure 1a). It has six square faces and eight hexagonal faces, comprised, respectively, of four- and six-member rings of edge-sharing polyhedra. The polyhedra are linked by peroxide bridges within the square rings, and these rings are joined by two bridging hydroxyl ligands at each juncture to form hexagonal rings. U_{24} remains one of the most readily formed clusters from a synthetic prospective: in geographically disparate labs, multiple single-crystal structures of U_{24} have been solved and refined with a variety of encapsulated species.[6] Although the hydroxyl ligand is ubiquitous in all but three (U_{20}, U_{28}, and U_{44}) of the ~40 uranyl POM clusters,[7] it has only recently been observed directly in a single-crystal X-ray structure,[8] and it has not been characterized by any other means. Herein, with the use of 2-dimensional (2D) multi-nuclear solid-state MAS NMR techniques and by the exploitation of encapsulated and lattice alkali species that are NMR-active nuclei, we capture detailed snapshots of the structure, solid-state dynamics, and chemical interactions between different parts of the uranyl POM capsules from outside to inside, namely, the lattice species, the uranyl shell, and the encapsulated alkali and aqua species.

The U_{24} subtypes for multinuclear solid-state NMR analyses were chosen strategically based on their NMR-active nuclei: a) $Li_2Na_{16}[Na_6(H_2O)_8][UO_2(O_2)(OH)]_{24}\cdot 72H_2O$ (Na-U_{24}; CSD-424819) reported recently, for which all encapsulated and charge-balancing species have been located,[5] b) the originally reported Li-U_{24},[3] (CSD-414640), for which the structural details with regard to encapsulated and lattice species have not been fully ascertained, and c) $Li_{18}[K_8Li_4(OH)_6][UO_2(O_2)(OH)]_{24}\cdot 76H_2O$ (LiK-U_{24}, CSD-426504), which is reported here for the first time with all encapsulated and charge-balancing species located. The encapsulated species as determined by single-crystal X-ray diffraction at 188 K for LiK-U_{24}, Na-U_{24}, and Li-U_{24} are illustrated in Figure 1b, c, and d, respectively.

Whereas Na-U_{24} and Li-U_{24} have alkali species located under the square face, the larger K^+ cations in LiK-U_{24} are located

[a] *Dr. T. M. Alam*
Department of Electronic, Optical and Nanostructured Materials
Sandia National Laboratories
Albuquerque, NM 87185 (USA)
E-mail: tmalam@sandia.gov

[b] *Dr. Z. Liao, Dr. L. N. Zakharov, Prof. M. Nyman*
Department of Chemistry and Materials Science of Actinides
Frontier Research Center
Oregon State University, Corvallis, OR 97331 (USA)
E-mail: May.Nyman@oregonstate.edu

Supporting information for this article is available on the WWW under http://dx.doi.org/10.1002/chem.201402351. It contains details of the syntheses and NMR characterization methodology used.

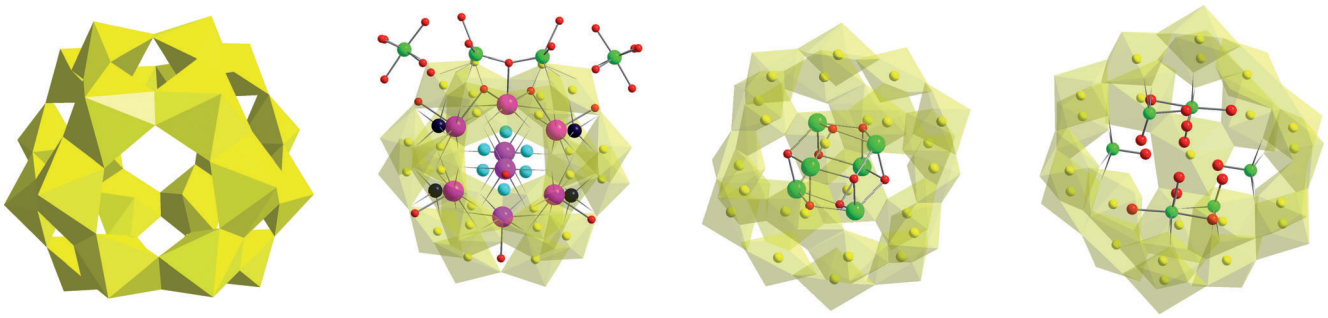

Figure 1. From left to right: a) U_{24}, $[UO_2(O_2)(OH)]_{24}^{24-}$ without any encapsulated species. b) LiK-U_{24} showing K^+ under the hexagonal faces (pink), Li^+ just inside four of the square faces (navy) bonded to the peroxide ligands, encapsulated OH^- (turquoise), and two coordination positions of Li^+ cations (light green) just outside of the hexagonal faces. Red spheres are water molecules. c) Na-U_{24} with Na^+ (green) under the six square faces bonded to $U=O_{yl}$, and water molecules under the hexagonal faces. d) Li-U_{24} with Li^+ (green) under two of the six square faces bonded to $U=O_{yl}$, and four additional encapsulated Li^+ cations (green) and their associated water molecules (red). Front uranyl polyhedra removed for ease of viewing in all three views of encapsulated species.

under the hexagonal face, an observation that is consistent with all prior computational and experimental studies that recognize the trend that small alkali species template square faces, medium-size alkali species template pentagonal faces, and large alkali species template hexagonal faces.[4a,c,d] The aqua species that coordinate K^+ are located under the square faces. The Li^+ cations occupying four of the six square faces have unprecedented coordination chemistry as they are bonded to the peroxide ligands instead of the internal yl-oxos. This places them nearly right on the boundary between the capsule interior and the external lattice. Surprisingly, all of the external charge-balancing Li^+ cations were located in the diffraction analysis of this new structure, a result that is unusual with the low Z of Li and the high disorder these phases exhibit, both in the lattice and inside the capsule. Both Na-U_{24} and Li-U_{24} have been described previously, but are summarized briefly for the sake of the discussion. In Na-U_{24}, Na^+ cations are bonded to the four O_{yl}=U in the six square faces and to the aqua species under the hexagonal faces. There are uncertainties in the encapsulated species in Li-U_{24} based on what is observed by X-ray diffraction. Two of the square faces host a Li^+ cation. There are two additional Li^+ cations that bridge two O_{yl}=U and bond four aqua species each, and two Li^+ cations each bonded to a water molecule, with suspect coordination (proximity to U^{6+} is ~2.6 Å).

Figure 2 compares the ^1H MAS NMR spectra of LiK-U_{24}, Na-U_{24}, and Li-U_{24} at reduced (278 K) and elevated (327 K) temperatures, with the ^1H NMR chemical shift assignments being summarized in Table S1 (see the Supporting Information). These ^1H NMR results clearly reveal the solid-state dynamic behavior of encapsulated aqua species, and that the rates of motion are a function of the encapsulated cluster cations. Variable-temperature (VT) ^1H MAS NMR spectra for LiK-U_{24}, Na-U_{24}, and Li-U_{24} are shown in Figures S1, S2 and S3, respectively (see the Supporting Information), with the relative exchange rates of the aqua species across the interface between encapsulated and lattice being in the order: LiK-U_{24} < Na-U_{24} < Li-U_{24} (details are provided below).

All ^1H NMR chemical shift assignments were based on homonuclear ^1H–^1H and heteronuclear ^1H–^7Li/^{23}Na NMR correlation

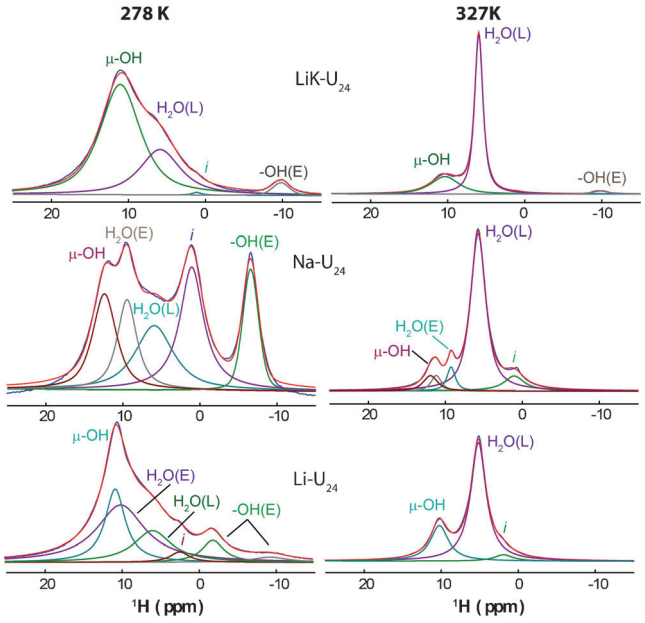

Figure 2. ^1H MAS NMR spectra of the different U_{24} materials at two different temperatures. The blue curve is the experimental curve and the red curve is the summation of calculated peaks. The different proton environments were identified: the bridging hydroxyls (μ-OH), lattice water ($H_2O(L)$), encapsulated water ($H_2O(E)$), encapsulated hydroxyl (−OH(E)), and an isolated water or phase impurity (*i*). Spectral assignments are discussed in the text and are summarized in Table S1 (see the Supporting information).

(HETCOR) experiments. All three U_{24} compositions revealed ^1H NMR chemical shifts between +9.5 and +12.5 ppm, which were assigned as either the μ_2-OH hydroxyl ligand or encapsulated water. Two μ_2-OH resonances were identified for Na-U_{24} whereas only one was observed for each of the Li-U_{24} and LiK-U_{24} samples. The downfield chemical shifts for μ_2-OH are consistent with ^1H NMR studies of model uranyl hydroxide materials, which will be highlighted in a future publication.

The 2D single quantum (SQ)–double quantum (DQ) ^1H MAS NMR correlation spectrum for Na-U_{24} (Figure 3a) reveals an autocorrelation peak for the μ_2-OH at $\delta = +11.2$ ppm with a set of DQ cross peaks (Figure 3b) between the

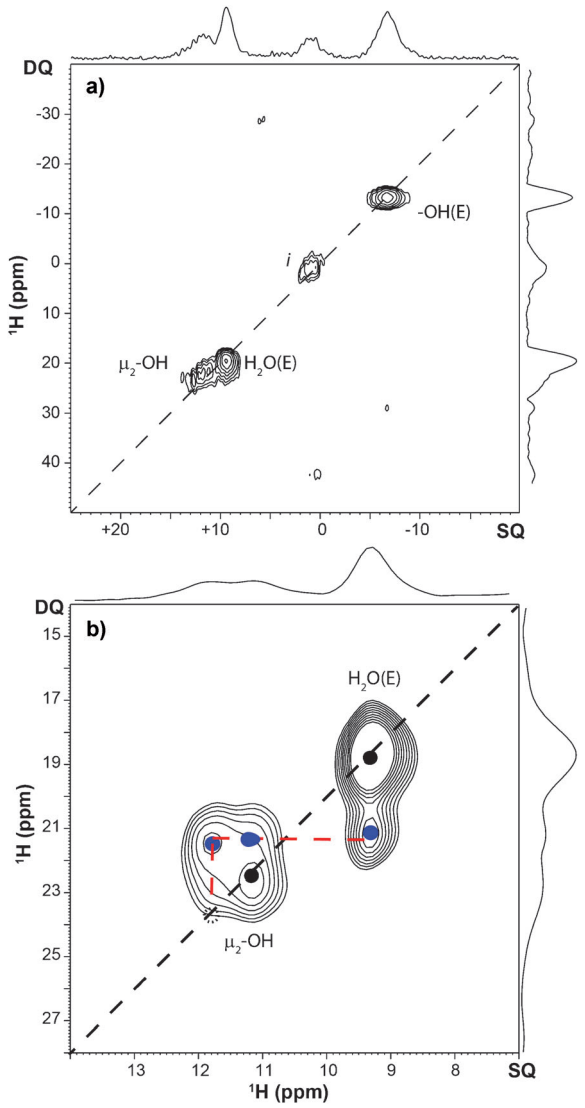

Figure 3. 2D DQ–SQ ^{1}H MAS NMR correlation spectrum for a) Na-U_{24} (327 K, $\tau_{DQ}=80$ μs) with spectral expansion of the μ_2-OH and H_2O(E) region (b). Autocorrelation peaks (●) and DQ cross peaks (blue ●) are shown, with the missing +12.0 ppm autocorrelation peak marked by a dashed circle, indicating no or weak autocorrelation for this environment.

$\delta=+12.0$ and +11.2 ppm that correspond to μ_2-OH resonances and an additional cross peak at $\delta=+9.2$ ppm assigned to the encapsulated water (H_2O(E)) resonance. No autocorrelation peak was observed for the +12.0 ppm resonance. In 2D ^{1}H–^{1}H DQ–SQ NMR correlation experiments, dipolar-derived autocorrelation peaks are observed for environments where protons with the same chemical shift are spatially close, $r(^{1}H–^{1}H)<5$ Å. DQ–SQ cross peaks arise when protons in different chemical environments (different chemical shifts) are spatially correlated. The lack of an autocorrelation peak for the μ_2-OH resonance at +12.0 ppm reveals that these types of hydroxyl ligands are >5 Å apart from each other, whereas the DQ–SQ cross peaks at $\delta=+11.2$ and 9.2 ppm reveal that the μ_2-OH ($\delta=+12$ ppm) species are <5 Å from H_2O(E) and the second μ_2-OH environment. Although the X-ray diffraction results do not resolve the orientation of the μ_2-OH ligands, external coordination to the capsule of lattice Na^+ necessitates two of the three μ_2-OH ligands located around the hexagonal face in the U_{24} cluster are pointed inward, and are probably hydrogen bonded to the H_2O(E), thus the +12.0 ppm chemical shift likely corresponds with the μ_2-OH pointed inwards. Conversely, the $\delta=+11.2$ μ_2-OH species are pointed outward, with no dipolar correlation with H_2O(E).

Similar NMR spectra showing the appearance of strong autocorrelation peaks for the μ_2-OH environments were also obtained for Li-U_{24} and LiK-U_{24}. The large positive chemical shift of the μ_2-OH capsule ligand was surprising and generally signifies acidity or hydrogen bonding for this proton in the crystalline state. It has been demonstrated the uranyl clusters are resistant to deprotonation, even in 2 M TMAOH (tetramethylammonium hydroxide) solution. Although mutual hydrogen bonding between hydroxyl ligands of two metal–oxo clusters has been shown to downshift the ^{1}H peak from ~2 ppm to >9 ppm,[9] the U_{24} capsules are always well separated in their lattice and never within mutual hydrogen-bonding distance, except for hydrogen bonding with lattice-based water molecules. The usual ^{1}H NMR chemical shift of a metal–oxo hydroxyl ligand is around 2 ppm. It may also be possible that local hydrogen bonding has shifted the pK_a of this hydroxyl in the solid state. It is also important to note that relativistic effects on the NMR chemical shifts in uranium complexes can vary significantly[10] and have not been extensively explored. The impact of relativistic effects on the NMR of uranyl materials are currently being investigated by computational methods.

Also present in the downfield region of the ^{1}H NMR spectra are the chemical shifts for encapsulated water molecules. For NaU_{24}, the assignment of the $\delta=+9.2$ ppm resonance as H_2O(E) is supported by the observation of a strong DQ autocorrelation peak arising from the water protons (Figure 3). H_2O(E) ($\delta=10.0$) is observed in Li-U_{24} only at reduced temperature, and none is observed in LiK-U_{24} at any temperature. However, LiK-U_{24} clearly has an aqua species that is located under the square face in the single-crystal structure (Figure 1), a species that we assign as an encapsulated hydroxyl, OH(E), with a corresponding chemical shift of −9.8 at both spectral temperatures. Assignment of this hydroxyl ligand also agreed with the charge balance, and with the ratio of μ_2-OH ligands and lattice water molecules. At low temperature, OH(E) species also become evident for Na-U_{24} (−6 ppm) and Li-U_{24} (−2 and −9.5 ppm); they are in rapid exchange with external aqua species at higher temperatures, which hinders their detection by significant peak broadening (see below). At higher temperatures, the resonance for the lattice water molecules, H_2O(L), dominates the ^{1}H NMR spectra for all U_{24} compositions and is observed at $\delta\approx+6$ ppm. The relative concentration of H_2O(L) and μ_2-OH peaks are in good agreement with that predicted from the structure. Inspection of the variable-temperature ^{1}H MAS NMR spectra (Figures S1–S3, see the Supporting Information) reveals that these environments are highly dynamic, and in the cases of Li-U_{24} and Na-U_{24}, involves exchange between H_2O(L) and the encapsulated hydroxyl species OH(E).

The H_2O(L) resonance is suppressed in the DQ NMR correlation spectra for all compounds owing to dynamic averaging of

the dipolar interaction, thereby allowing observation of the more minor peaks. As the temperature is reduced towards freezing, the $H_2O(L)$ resonance broadens owing to reduced spin–spin T_2 relaxation, resulting from slowing of the lattice water molecule motions. At higher temperatures, chemical shift averaging occurs between $H_2O(L)$ and OH(E), giving rise to a single dominant water resonance with no observable OH(E) resonance between 0 and −15 ppm for all but LiK-U_{24} (Figure 2). The VT ^{1}H MAS NMR spectra for Na-U_{24} allows the timescale for the exchange between OH(E) and $H_2O(L)$ to be estimated. The peak separation ($\Delta\delta$) between the $H_2O(L)$ and OH(E) resonances is ~7500 Hz, meaning that the exchange rate ($k=\pi\delta\triangle/\sqrt{2}$) must be faster than ~17 kHz at temperatures above 313 K. Similarly, for Li-U_{24}, k must be >25 kHz above 313 K. For the LiK-U_{24} material, the appearance of a distinct −OH(E) ^{1}H NMR resonance over the entire temperature range requires that the exchange rate is significantly smaller than ~15 kHz. The relative order of the hydrogen exchange rate for the encapsulated environment is thus KLi-U_{24} ≪ Na-U_{24} < Li-U_{24}.

Although the 2D DQ–SQ NMR correlation experiments are powerful, they do not provide any details about the proximity of the $H_2O(L)$ protons to the other environments owing to the motional averaging of the dipolar coupling for this species. 2D ^{1}H MAS NMR NOESY spectra (Figure 4) allow these $H_2O(L)$ spatial correlations to be explored. For all of the U_{24} compositions investigated, a strong magnetization exchange between the OH(E) (between −5 and −10 ppm) and $H_2O(L)$ ($\delta=+5.8$ ppm) was observed. For Na-U_{24} (Figure 4a) and Li-U_{24}, lower temperatures were required to prevent the dynamic averaging of the OH(E), whereas in KLi-U_{24} (Figure 4b), OH(E) correlations are still distinguishable at higher temperatures.

MAS NMR spectroscopy of the ^{23}Na and ^{7}Li cations further confirms the location of the different ^{1}H species, but also provides additional insight about the solid-state dynamic behavior of the capsules. As previously described, the Na-U_{24} ^{23}Na MAS NMR spectra (Figure S5, in the Supporting Information) shows two environments assigned to the lattice Na ($\delta=-3.8$ ppm) and the encapsulated Na ($\delta=-25.8$ ppm), with a lattice/encapsulated ratio of 2.3, an observation that is consistent with the ratio of 2.7 predicted from X-ray diffraction studies.[5] The ^{1}H–^{23}Na MAS NMR HETCOR spectrum (298 K) is shown in Figure 5a, with the encapsulated Na dipolar coupled to the $H_2O(E)$ ($\delta=-6.1$ ppm). The lattice Na is not observed owing to dynamics. Interestingly, at temperatures above 313 K, the 2D HETCOR (Figure S6, in the Supporting Information) shows a correlation shift to the motionally averaged ^{1}H resonance at $\delta\approx6$ ppm, reflecting the ^{1}H chemical shift averaging between $H_2O(E)$ and $H_2O(L)$ at elevated temperatures, as discussed above. No correlations were observed between the encapsulated Na environment and the μ_2-OH at the hexagonal face, further supporting the X-ray diffraction observation that the encapsulated Na species are well-confined inside the capsule.

The ^{7}Li MAS NMR spectrum (Figure S7, in the Supporting Information) for Na-U_{24} ($Li_2Na_{16}[Na_6(H_2O)_8][UO_2(O_2)(OH)]_{24}\cdot72H_2O$) shows a resonance for lattice Li species ($\delta=1.3$ ppm) as predicted, but also reveals that ~1% of the Li is encapsulated ($\delta=-10.6$ ppm), showing the possibility of minor Li disorder to the internal encapsulated $Na_2(H_2O)_8$ refined by X-ray diffraction. The 2D ^{1}H–^{7}Li MAS NMR HETCOR spectrum for Na-U_{24} (Figure S8, in the Supporting Information) reveals contact between the lattice Li species and the $H_2O(L)$ as expected, but also dipolar interaction with μ_2-OH, suggesting that Li is partially associated near the cluster hexagonal face.

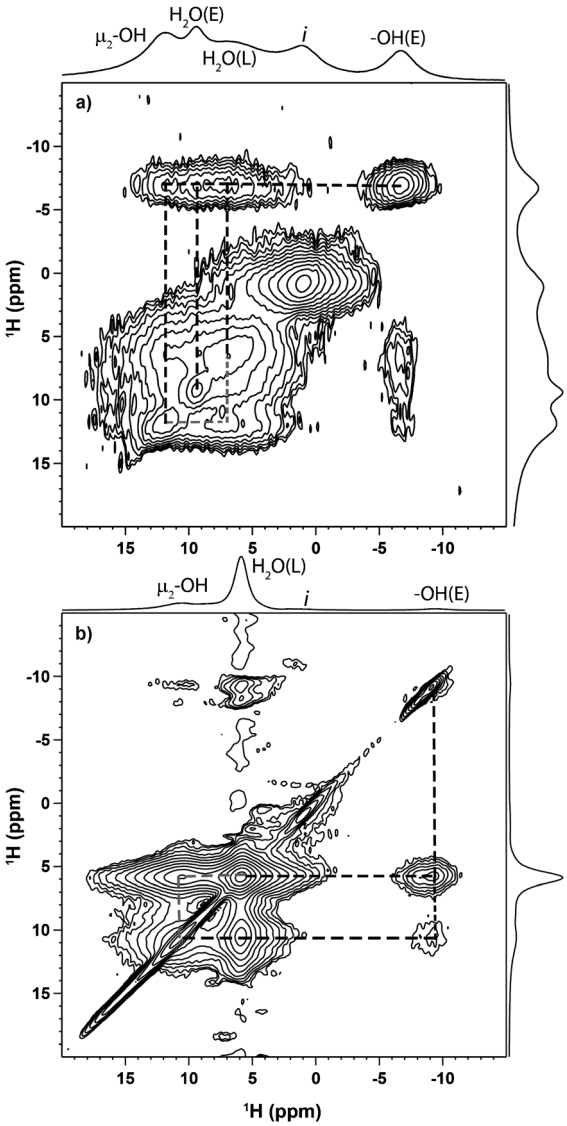

Figure 4. 2D ^{1}H MAS NMR NOESY spectra for a) the Na-U_{24} cluster (293 K, $\tau_{mix}=1$ ms) and b) the KLi-U_{24} (323 K, $\tau_{mix}=10$ ms).

For the LiK-U_{24} compound, the ^{7}Li MAS NMR spectrum shows a lattice Li environment ($\delta\approx0$ ppm) and an encapsulated Li environment ($\delta=-13.9$ ppm). In this capsule, the 2D ^{1}H–^{7}Li MAS NMR HETCOR spectrum (Figure 5b) shows the strong cross peak between the encapsulated Li (−13.8 ppm) and −OH(E) ($\delta=-9.8$ ppm), and a slightly weaker cross peak involving the μ_2-OH. In this structure, like Na-U_{24}, the lattice Li^+ ions bonded to the exterior of the capsule may force these μ_2-OH ligands to point inward. 2D ^{7}Li–^{7}Li (LiK-U_{24}) and ^{23}Na–^{23}Na (Na-U_{24}) MAS NMR exchange experiments also demonstrate ex-

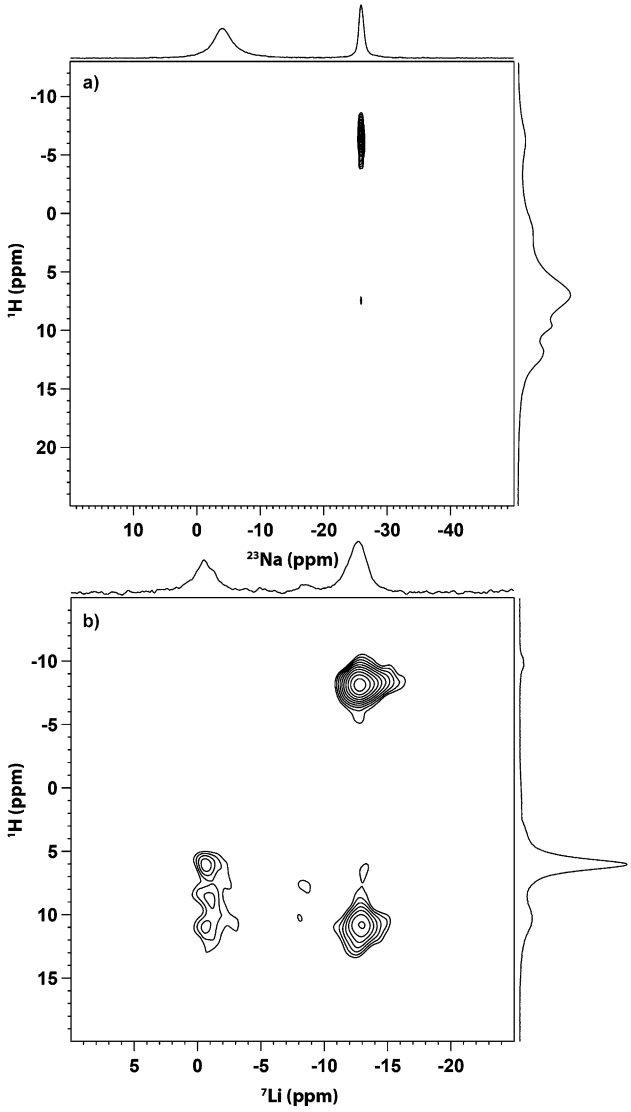

Figure 5. 2D MAS NMR HETCOR spectra: a) ^{1}H–^{23}Na HETCOR for Na-U_{24} and b) ^{1}H–^{7}Li HETCOR for LiK-U_{24}.

change of the cations between the encapsulated and lattice environments in the solid state on the ms time scale (Figure S8).

Chemical shift averaging is apparent in the VT ^{7}Li MAS NMR spectrum of Li-U_{24}, which shows two overlapping environments at +0.3 and −2.9 ppm, both chemical shifts consistent with Li associated with lattice water molecules. However, as the temperature is reduced, an encapsulated Li^+ environment (−13 ppm) becomes resolved (Figure S9, in the Supporting Information). This averaging represents a multisite exchange process, and was not readily simulated without additional constraints. The collapse of the line shape to a single resonance requires the Li exchange rate $k > 8$ kHz. Compare this to LiK-U_{24}, which at 328 K shows both resonances for the lattice Li (~0 ppm) and the encapsulated Li ($\delta = -13$ ppm), an observation that places a restriction of the Li exchange being $\ll 8$ kHz. The relative order of the Li exchange rate is thus KLi-$U_{24} \ll$ Li-U_{24}, which mirrors the encapsulated aqua species exchange rates. These dynamics were also prevalent during solution ^{7}Li NMR experiments wherein aqueous solutions of LiK-U_{24} and Li-U_{24} revealed only a single dynamically averaged resonance, with no encapsulated Li^+ environment observed. The current results combined with previous exchange-dynamics studies of Na-U_{24} and related U_{28} clusters[5] all agree that in both solution and the solid state, larger encapsulated alkali species slow the exchange of all the encapsulated species. This suggests a concerted motion amongst the species occurs in the capsule interior, and the alkali species exit through the larger faces (i.e., hexagons vs. squares). It is especially pertinent if we consider the solid-state (low-temperature) location of the Li^+ ion in LiK-U_{24}, just underneath the square face, almost outside it: because the smallest dimension of the square face (the O to O distance) is < 3.8 Å, and in the solid state the faces are probably far less flexible than in solution, this Li^+ ion is likely fixed in that it cannot easily access the hexagonal face that is blocked by the interior OH(E) and K^+ ion. Similarly, we do not observe OH(E) exchange because it is also blocked.

This solid-state NMR study adds considerably to the growing and emerging body of knowledge of actinide clusters, and more broadly actinide chemistry at all length scales from monomers to infinite solids. The NMR data provides characterization of the hydrogen environment for the μ_2-OH proton that is common to many aqueous and solid-state uranyl POM chemistries. These studies also reveal previously undetected encapsulated hydroxyl species and how they are associated with encapsulated alkali species. These encapsulated hydroxyl, water, and cation species may also be present in many of the known uranyl peroxide capsules, and are shown to be readily distinguishable by NMR spectroscopy. The surprisingly high room-temperature mobility of Li^+ in the solid state between the encapsulated and lattice positions supports the role of cation size in the proposed mechanisms of ion exchange in uranyl POMs and in other related capsule-like POMs.[11] Finally, we are inspired to advance studies of capsule environments towards new materials for energy applications such as solid-state ion conductors. The electronically and chemically fascinating UO_2^{2+} ion continues to bring forth new discoveries that will result in unprecedented clusters and materials and their application in nuclear and other alternative energy applications.

Acknowledgements

This work was supported as part of the Materials Science of Actinides, an Energy Frontier Research Center funded by the Department of Energy, Office of Science, Office of Basic Energy Sciences under award number DE-SC0001089. The NMR component of the work (T.M.A.) was performed at Sandia National Laboratories, which is a multiprogram laboratory managed and operated by Sandia Corporation, a wholly owned subsidiary of Lockheed Martin company, for the U. S. Department of Energy's National Nuclear Security Administration under contract DE-AC04–94AL85000.

Keywords: ion-exchange · polyoxometalate · proton MAS NMR · solid-state NMR · uranyl

[1] J. R. Winkler, H. B. Gray, *Struct. Bonding (Berlin)* **2011**, *142*, 17 – 28.
[2] a) A. Neyman, L. Meshi, L. Zeiri, I. A. Weinstock, *J. Am. Chem. Soc.* **2008**, *130*, 16480; b) Y. F. Wang, I. A. Weinstock, *Chem. Soc. Rev.* **2012**, *41*, 7479 – 7496; c) Y. F. Wang, O. Zeiri, S. Sharet, I. A. Weinstock, *Inorg. Chem.* **2012**, *51*, 7436 – 7438.
[3] P. C. Burns, K. A. Kubatko, G. Sigmon, B. J. Fryer, J. E. Gagnon, M. R. Antonio, L. Soderholm, *Angew. Chem.* **2005**, *117*, 2173 – 2177; *Angew. Chem. Int. Ed.* **2005**, *44*, 2135 – 2139.
[4] a) A. Gil, D. Karhanek, P. Miro, M. R. Antonio, M. Nyman, C. Bo, *Chem. Eur. J.* **2012**, *18*, 8340 – 8346; b) P. Miro, C. Bo, *Inorg. Chem.* **2012**, *51*, 3840 – 3845; c) P. Miro, S. Pierrefixe, M. Gicquel, A. Gil, C. Bo, *J. Am. Chem. Soc.* **2010**, *132*, 17787 – 17794; d) M. Nyman, M. A. Rodriguez, T. M. Alam, *Eur. J. Inorg. Chem.* **2011**, 2197 – 2205; e) B. Vlaisavljevich, L. Gagliardi, P. C. Burns, *J. Am. Chem. Soc.* **2010**, *132*, 14503 – 14508.
[5] M. Nyman, T. M. Alam, *J. Am. Chem. Soc.* **2012**, *134*, 20131 – 20138.
[6] Personal communication with Professor Peter Burns at Notre Dame University, Indiana, USA.
[7] a) M. Nyman, P. C. Burns, *Chem. Soc. Rev.* **2012**, *41*, 7354 – 7367; b) J. Qiu, P. C. Burns, *Chem. Rev.* **2013**, *113*, 1097 – 1120.
[8] P. L. Zanonato, P. Di Bernardo, A. Fischer, I. Grenthe, *Dalton Trans.* **2013**, *42*, 10129 – 10137.
[9] M. Nyman, T. Alam, F. Bonhomme, M. Rodriguez, C. Frazer, M. Welk, *J. Cluster Sci.* **2006**, *17*, 197 – 219.
[10] a) G. Schreckenbach, S. K. Wolff, T. Ziegler, *J. Phys. Chem. A* **2000**, *104*, 8244 – 8255; b) G. Schreckenbach, *Inorg. Chem.* **2002**, *41*, 6560 – 6572; c) P. Hrobárik, V. Hrobáriková, A. H. Greif, M. Kaupp, *Angew. Chem.* **2012**, *124*, 11042 – 11046; *Angew. Chem. Int. Ed.* **2012**, *51*, 10884 – 10888.
[11] a) A. Merca, E. T. K. Haupt, T. Mitra, H. Bogge, D. Rehder, A. Muller, *Chem. Eur. J.* **2007**, *13*, 7650 – 7658; b) A. Müller, Y. S. Zhou, H. Bogge, M. Schmidtmann, T. Mitra, E. T. K. Haupt, A. Berkle, *Angew. Chem.* **2006**, *118*, 474 – 479; *Angew. Chem. Int. Ed.* **2006**, *45*, 460 – 465.

Received: February 25, 2014
Published online on May 30, 2014